Journal Code:				Article ID				Dispatch: 28.09.12	CE: Zolamarie Z. Zamudio
E	T	T		2	5	9	1	No. of Pages: 9	ME:

TRANSACTIONS ON EMERGING TELECOMMUNICATIONS TECHNOLOGIES
Trans. Emerging Tel. Tech. (2012)
Published online in Wiley Online Library (wileyonlinelibrary.com). DOI: 10.1002/ett.2591

RESEARCH ARTICLE

Hierarchical underwater acoustic sensor networks with (virtual) transmit/receive arrays

Andrej Stefanov[1]* and Milica Stojanovic[2]

[1] Information Technology Department, IBU Skopje, Skopje, Macedonia
[2] Electrical and Computer Engineering Department, Northeastern University, Boston, MA, USA

ABSTRACT

We consider a hierarchical underwater acoustic sensor network architecture in which the sensors and the collector stations operate in distinct layers. The hierarchical architecture is motivated by the property of the acoustic underwater transmission medium that for each transmission distance, there exists an operating frequency for which the narrow-band signal-to-noise ratio is maximised. The sensors and the collector stations are consequently allocated different operating frequencies. We assume a uniform distribution of both sensors and collector stations over the finite area of the sensing field. The sensors are organised into clusters forming virtual transmit/receive arrays. The collector stations, on the other hand, are equipped with co-located transmit/receive arrays. We adopt a communication-theoretic approach and study the interdependence of the sustainable number of hops through the network, end-to-end frame error probability, power and bandwidth allocation. The analysis is performed under the assumption of Ricean fading and interference from other nodes within the same layer of the hierarchy. We present numerical examples that illustrate the network performance and demonstrate that there are preferred operating frequencies, which ensure network operation without any cross-interference between the collector network and the sensor network. Copyright © 2012 John Wiley & Sons, Ltd.

***Correspondence**
Andrej Stefanov, Information Technology Department, IBU Skopje, Skopje, Macedonia.
E-mail: andrejstefanov@ieee.org

Received 23 September 2011; Revised 26 August 2012; Accepted 4 September 2012

1. INTRODUCTION

The design and analysis of underwater wireless (acoustic) communications systems is receiving an increased interest by both researchers and practitioners in the area [1, 2]. Initial research efforts have focused on underwater acoustic channel modelling and point-to-point communications [3, 4]. Motivated by these theoretical models and driven by the maturation of underwater acoustic modem technology [5, 6], the development of underwater sensor networks is coming close to realisation [7].

In this paper, we investigate a hierarchical sensor network architecture in which the sensors and the collector stations operate in distinct layers. The architecture draws on the salient characteristics of acoustic propagation. Namely, it exploits the frequency-dependent attenuation, which exhibits the property that for each transmission distance, there exists an operating frequency for which the narrowband signal-to-noise ratio is maximised. We envision an underwater network of bottom-mounted nodes and a two-dimensional network topology. The bottom-mounted nodes are battery powered, which means that power efficiency represents an important consideration in the network design. Hence, we consider a network where the nodes are organised into clusters, which allows the application of the virtual (distributed) transmit/receive arrays concept [8, 9] along with cooperative (distributed) space–time coding [10, 11]. This represents an appealing alternative to standard multihop transmission, because by utilising suitable signal processing techniques, the virtual transmit/receive arrays have the potential to deliver the power savings and rate/reliability benefits of multiple-input multiple-output systems. In addition to the power-limited nodes, underwater acoustic communication systems are characterised by the power that is subject to high attenuation, which depends on both the distance and the frequency of the signal, and the bandwidth, which is severely limited. Thus, we consider a multihop transmission protocol based on nearest-neighbour cluster-to-cluster routing that offers more promising bandwidth and path loss conditions. As the physical layer plays such a prominent role, a bottom-up approach emerges as a natural choice in the study of underwater acoustic networks. Hence, we adopt a communication-theoretic approach [12] and investigate the

network performance in the presence of interference from other clusters in the network. The cluster-to-cluster channel is subject to frequency-dependent path loss and Ricean fading. This study focuses on the interdependence between the sustainable number of cluster-to-cluster hops in the network, as an indicator of network connectivity; end-to-end frame error probability; power; and bandwidth allocation.

This paper is organised as follows. Section 2 describes an underwater acoustic propagation model. Section 3 introduces the hierarchical sensor network architecture and presents the communication-theoretic analysis of underwater acoustic clustered sensor networks utilising virtual transmit/receive arrays. Numerical examples illustrating the results of the analysis are presented in Section 4. Section 5 concludes this paper.

2. UNDERWATER ACOUSTIC PROPAGATION

Underwater acoustic communication channels are characterised by a path loss that depends not only on the distance between the transmitter and the receiver, as is the case in many other wireless channels, but also on the signal frequency. The absorption loss increases with frequency, as well as with distance. It imposes a limit on the available bandwidth, because of the practical constraints of finite transmission power.

2.1. Attenuation

Attenuation, or path loss, which occurs in an underwater acoustic channel over a distance d for a signal of frequency f, is given by

$$A(d, f) = A_0 d^{\kappa} a(f)^d \tag{1}$$

where A_0 is a unit-normalising constant, $a(f)$ is the absorption coefficient and κ is the spreading factor. In the case of practical spreading, $\kappa = 1.5$. The absorption coefficient, which is an increasing function of frequency, can be expressed empirically using Thorp's formula, which gives $a(f)$ in decibel per kilometre for f in kilohertz as [13]

$$10 \log a(f) = \frac{0.11 f^2}{1 + f^2} + \frac{44 f^2}{4100 + f^2} + \frac{2.75 f^2}{10^4} + 0.003 \tag{2}$$

This formula is generally valid for frequencies above a few hundred hertz.

2.2. Noise

The ambient noise in the ocean comes from diverse sources (turbulence, shipping, waves and thermal noise), which can be described by Gaussian statistics and a continuous power spectral density (p.s.d.). The following empirical formulae

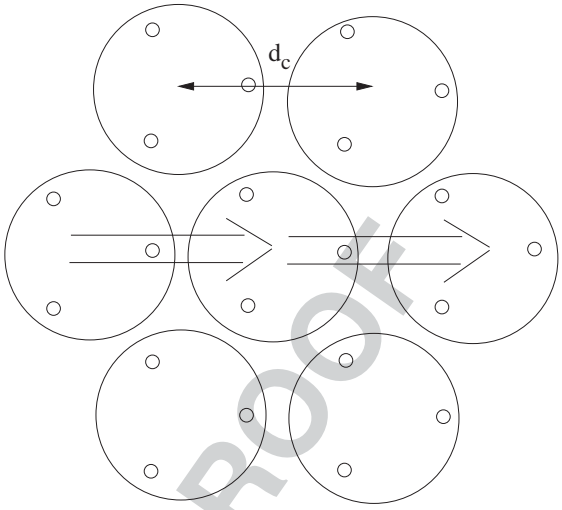

Figure 1. Cluster-to-cluster transmission with $N_c = 3$ nodes per cluster. The distance between neighbouring clusters is d_c.

give the p.s.d.'s of the four noise components in decibel relative to micropascal per hertz* as a function of frequency in kilohertz [13]:

$$\begin{aligned} 10 \log N_t(f) &= 17 - 30 \log f \\ 10 \log N_s(f) &= 40 + 20(s - 0.5) + 26 \log f \\ &\quad - 60 \log(f + 0.03) \\ 10 \log N_w(f) &= 50 + 7.5\sqrt{w} + 20 \log f - 40 \log(f + 0.4) \\ 10 \log N_{th}(f) &= -15 + 20 \log f \end{aligned} \tag{3}$$

where s is the shipping activity factor, $0 \leqslant s \leqslant 1$, and w is the wind speed in metre per second. The overall p.s.d. of the ambient noise is

$$N(f) = N_t(f) + N_s(f) + N_w(f) + N_{th}(f) \tag{4}$$

3. HIERARCHICAL SENSOR NETWORK

We consider a hierarchical sensor network architecture. The bottom-mounted sensors constitute the first layer in the architecture. The sensors are organised into disjoint cells. The sensors in each cell are organised into clusters forming virtual (distributed) transmit/receive arrays. They communicate their information by utilising cluster-to-cluster multihop relaying along nearest-neighbour clusters as depicted in Figure 1. The information is communicated to the collector station located at the centre of the cell. The collector stations (collectors), which are also bottom mounted,

*Note that an acoustic signal propagates as a pressure wave whose level is commonly measured in decibel relative to 1 μPa.

Trans. Emerging Tel. Tech. (2012) © 2012 John Wiley & Sons, Ltd.
DOI: 10.1002/ett

form the second layer in the hierarchical architecture. The collector stations, equipped with co-located transmit/receive arrays also utilise multihop relaying to transmit their respective information to the central collector. As the distance between the sensors is shorter than the distance between the collectors, the sensor cluster-to-cluster transmissions are allocated a higher operating frequency than the collector-to-collector transmissions.

3.1. Data gathering protocol

Both the sensors and the collectors utilise the same data gathering protocol. The difference is that the sensors are organised into clusters. We consider two versions of the protocol and describe it in terms of sensor's clustered transmissions to the collector.

Protocol 1: The protocol is illustrated in Figure 2. The sensor clusters closest to the collector transmit their information first in a single-hop transmission to the collector as depicted in Figure 2(c). The sensor clusters that are two hops away transmit next through a two-hop route to the collector and so on. As they need to relay the data, the sensor clusters closer to the collector can take advantage of the established route and transmit again. For example, Figure 2(a) shows sensor clusters that are three hops away from the collector. They establish three-hop routes. The other sensor clusters in the route, which are within two hops and a single hop from the collector, take advantage of the established route and send new information to the collector.

We note that a form of spatial reuse is possible, where in each time slot, some nodes can simultaneously transmit on the same frequency band [14]. Of course, this leads to interference among transmissions utilising the same time slot and the same bandwidth.

Protocol 2: The second data gathering protocol is a simplified version of the protocol described previously. In this case, the sensor clusters still utilise multihop transmissions; however, all sensor clusters that are within the collector's cell transmit only once to the collector. In other words, sensor clusters closer to the collector that are part of a multihop route for a sensor cluster that is farther away from the collector only act as relays and do not transmit new information to the collector.

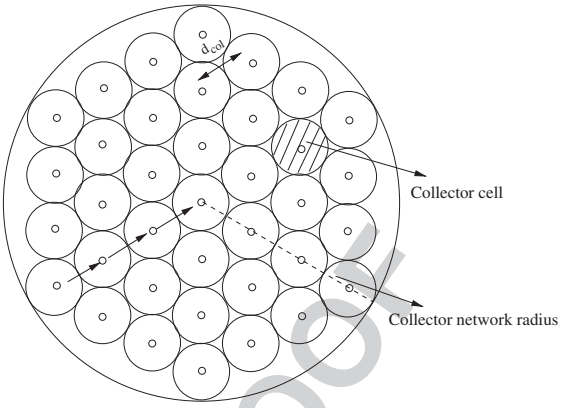

Figure 3. Network of collector stations.

3.2. Collector network topology

We consider a network of bottom-mounted collector stations. Therefore, we focus on a two-dimensional network that provides coverage over a certain area. Let the area of the network be a circle of radius r. We assume a uniform distribution of collector stations in the network as depicted in Figure 3. Given the number of collector stations in the network, K, and the area of the network, $\mathcal{A}$, the density of the collector stations in the network is

$$\rho_{\text{col}} = \frac{K}{\mathcal{A}} \tag{5}$$

For a uniform collector station distribution, the distance between the collector stations is

$$d_{\text{col}} = \frac{c}{\sqrt{\rho_{\text{col}}}} \tag{6}$$

where c is a constant that depends on the node placement (grid pattern). Without the loss of generality, we assume that $c = 1$.

We assume multihop transmission based on nearest-neighbour routing. This is an energy saving strategy, and as such, it may be attractive for networks with limited energy, battery-powered nodes. The analysis is performed under the assumption that the route between the source and the destination is known. Further discussion regarding route

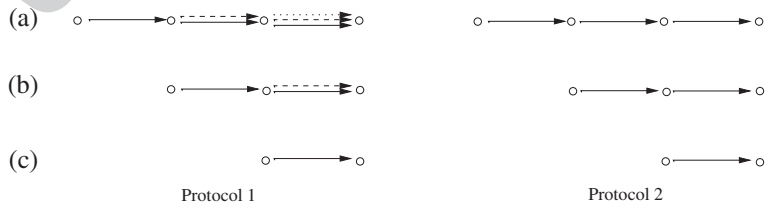

Figure 2. Data gathering protocol. In the first version of the protocol, Protocol 1, clusters that are within an established route take advantage of the established route and send new information to the collector. In the second version of the protocol, Protocol 2, clusters that are within an established route simply act as relays and do not send new information to the collector.

discovery and the exchange of control messages may be found in [12] and references therein. As the longest multihop route in the network is along the radius of the network r, the maximum number of collector-to-collector hops is

$$n_{\mathrm{c}}^{\max} = \frac{r}{d_{\mathrm{col}}} = \frac{\sqrt{\mathcal{A}/\pi}}{\sqrt{\mathcal{A}/K}} = \sqrt{\frac{K}{\pi}} \tag{7}$$

3.3. Sensor network topology

We consider a network of bottom-mounted sensors. We assume a uniform distribution of N sensors in the network. As there are K collector stations, there are $M_{\mathrm{c}} = N/K$ sensors per collector station, as depicted in Figure 4. The coverage area (cell) of each collector is $\mathcal{A}_{\mathrm{c}}$. Hence, the density of the sensors is

$$\rho_{\mathrm{s}} = \frac{M_{\mathrm{c}}}{\mathcal{A}_{\mathrm{c}}} = \frac{N}{K\mathcal{A}_{\mathrm{c}}} \approx \frac{N}{\mathcal{A}} = \frac{1}{d_{\mathrm{s}}^2} \tag{8}$$

where d_{s} denotes the distance between sensors.

We assume that groups of N_{c} sensors are organised into clusters. The density of clusters in a cell is

$$\rho_{\mathrm{c}} = \frac{M_{\mathrm{c}}/N_{\mathrm{c}}}{\mathcal{A}_{\mathrm{c}}} = \frac{\rho_{\mathrm{s}}}{N_{\mathrm{c}}} \tag{9}$$

We define the distance between clusters, d_{c}, as the distance between the centres of the clusters. Hence,

$$d_{\mathrm{c}} = d_{\mathrm{s}}\sqrt{N_{\mathrm{c}}} \approx \sqrt{\frac{N_{\mathrm{c}}}{\rho_{\mathrm{s}}}} \tag{10}$$

We assume cluster-to-cluster multihop routes along nearest-neighbour clusters, as depicted in Figure 5. Following the steps of Section 3.2, we obtain the maximum number of sensor cluster-to-cluster hops as

$$n_{\mathrm{s}}^{\max} = \frac{1}{\sqrt{\pi}}\sqrt{\frac{N}{N_{\mathrm{c}}K}} \tag{11}$$

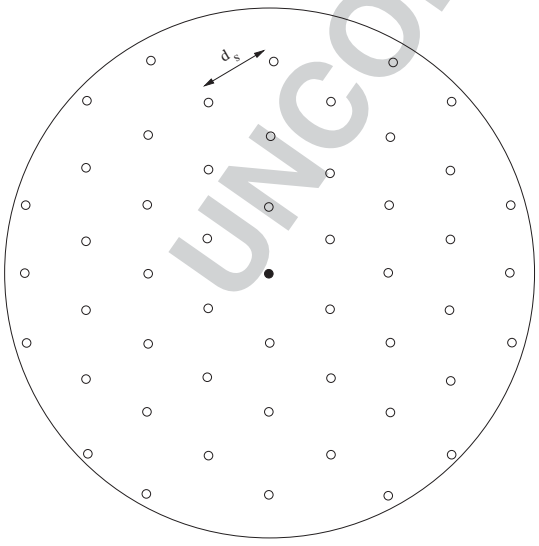

Figure 4. A collector cell contains $M_c = \frac{N}{K}$ sensors.

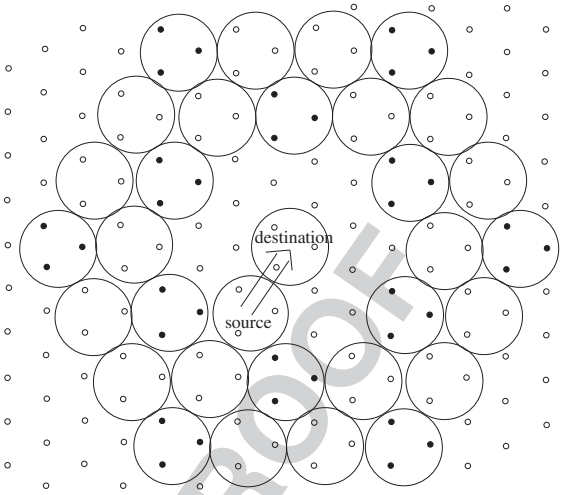

Figure 5. Interfering clusters in the network.

3.4. Interference model

In order to illustrate the interference model, we focus on a single transmission from a source cluster to a destination cluster, as depicted in Figure 5. We impose a protocol constraint: no clusters that are at the same distance from the destination cluster as the source cluster are allowed to transmit in the same time slot and in the same frequency band as the source during the source cluster's transmission.

The remaining clusters that may interfere with the source cluster's transmission are organised in tiers. As we assume hexagonal topology, there will be at most 12 interfering clusters in tier 1, 18 interfering clusters in tier 2, and so on. A scenario where all other clusters in the network transmit at the same time would be unrealistic, as we also need to consider that there need to be some receiving clusters in the network. Figure 5 depicts a scenario where half of the clusters in tier 1 and a third of the clusters in tier 2 transmit at the same time and in the same frequency band as the source, therefore creating interference. Note that because the clusters in tier 2 are farther away, their impact is less pronounced. Assuming all clusters transmit at some constant p.s.d. level S, the interference from the clusters in the first and second tiers is

$$I(f) \approx \frac{c_1 S}{A(2d_{\mathrm{c}}, f)} + \frac{c_2 S}{A(3d_{\mathrm{c}}, f)} \tag{12}$$

where $c_1 \leqslant 12$ and $c_2 \leqslant 18$ are constants indicating the number of interfering clusters in tiers 1 and 2, respectively. In particular, we let $c_1 = c_2 = 6$. As there are

Trans. Emerging Tel. Tech. (2012) © 2012 John Wiley & Sons, Ltd.
DOI: 10.1002/ett

multiple interfering clusters in the network, we assume that the interference is Gaussian with a p.s.d. given by Equation (12).

Using the attenuation $A(d, f)$, the noise p.s.d. $N(f)$ and the interference p.s.d. $I(f)$, we can evaluate the signal-to-interference-plus-noise ratio (SINR) observed over a distance d_c, as shown in Figure 6. We observe that there is a preferred operating frequency, $f_o(d_c)$, which depends on the distance, d_c, where $[A(d_c, f)(N(f) + I(f))]^{-1}$ is maximised. Figure 7 presents this preferred operating frequency, $f_o(d_c)$, as a function of the distance, given transmit p.s.d. level of $S = 110$ dB re μPa per Hz for f in kilohertz. We note that the preferred operating frequency is higher when there is interference. Figure 8 presents this preferred operating frequency as a function of the transmit p.s.d. for various distances.

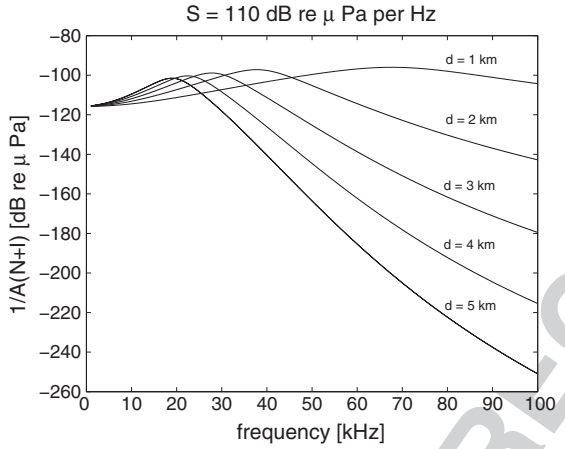

Figure 6. $[A(N+I)]^{-1}$ for various distances. The power spectral density is $S = 110$ dB re μPa per Hz. The spreading factor is $\kappa = 1.5$.

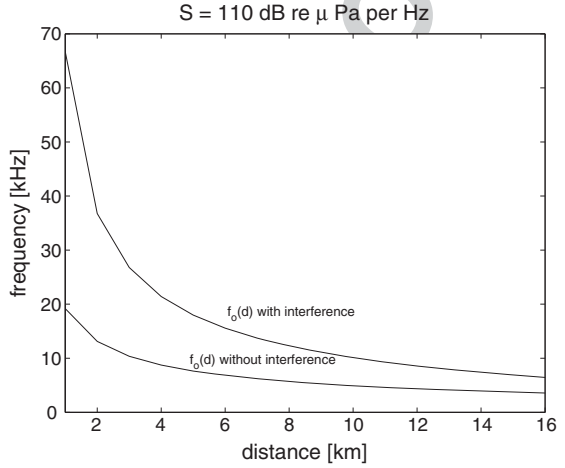

Figure 7. Operating frequency versus distance for transmit power spectral density of $S = 110$ dB re μPa per Hz. The spreading factor is $\kappa = 1.5$.

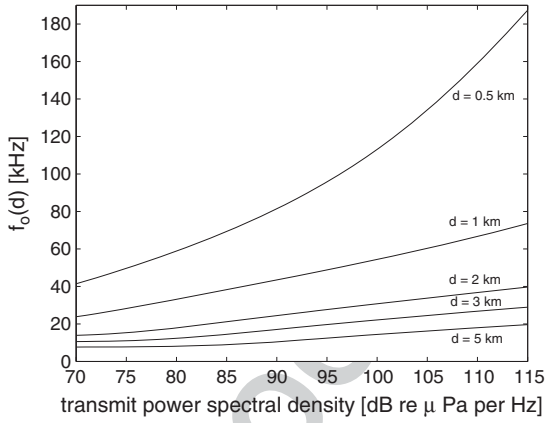

Figure 8. Operating frequency with interference versus transmit power spectral density for various distances. The spreading factor is $\kappa = 1.5$.

3.5. Multihop transmission

We assume a simple (distributed) space–time block code with a decode-and-forward strategy employed by the relays. The end-to-end frame error probability for a multihop route with n_h cluster-to-cluster hops is given by

$$p_{\text{route}} = 1 - (1 - p_b)^{Ln_h} \tag{13}$$

where p_b denotes the bit error probability of a single cluster-to-cluster link and L denotes the frame size in bits.

We consider the quality of service for the network in terms of the maximum allowed end-to-end route frame error probability, that is, we require $p_{\text{route}} \leqslant p_{\text{route}}^{\max}$. Let the number of cluster-to-cluster hops that can be sustained by the network, that is, the number of cluster-to-cluster hops that can satisfy the maximum end-to-end route frame error probability, be denoted by n_{sh}. From Equation (13), it follows that n_{sh} can be calculated as[†]

$$n_{sh} = \frac{1}{L}\frac{\log\left(1 - p_{\text{route}}^{\max}\right)}{\log(1 - p_b)} \approx \frac{1}{L}\frac{p_{\text{route}}^{\max}}{p_b} \tag{14}$$

Under the assumption of a Ricean fading model for the (cluster-to-cluster) communication channel [15, 16], and assuming that perfect channel state information is available at the receiver, the bit error probability, p_b, can be approximated as [17]

$$p_b \lesssim \left(\frac{1 + \mathcal{K}}{1 + \mathcal{K} + \gamma(d_c, f)}\right)^{tr} \exp\left(-\frac{tr\mathcal{K}\gamma(d_c, f)}{1 + \mathcal{K} + \gamma(d_c, f)}\right) \tag{15}$$

where $\mathcal{K}$ denotes the Ricean fading factor assumed to be the same for all node-to-node sub-channels, t denotes the

[†]Note that although the analysis does not consider it explicitly, in practice, $\{n_{sh}, n_c \max, n_s^{\max}\} \in \mathbb{N}$.

transmit diversity gain, r denotes the receive diversity gain and γ denotes the SINR. We assume that the attenuation, noise and interference are constant over the entire bandwidth, so that the SINR can be calculated as

$$\gamma(d_c, f) = \frac{P}{A(d_c, f)(N(f) + I(f))B} \tag{16}$$

where B is the bandwidth in kilohertz and P is the transmit power.

The frequency-nonselective assumption is a suitable approximation for systems with narrow bandwidth. It can also be extended to wideband multicarrier systems, such as orthogonal frequency-division multiplexing [18]. In that case, the operating frequency, $f_o(d_c)$ would describe the performance on one of the carriers. The performance on the other carriers would correspond to the frequency $f_o(d_c)$ shifted by multiples of subcarrier separation Δf.

4. NUMERICAL EXAMPLES

We present numerical examples to examine the relationships between the sustainable number of hops, the end-to-end frame error probability, signal power and bandwidth. We assume Ricean fading for each channel [15, 16]. The Ricean fading factor is taken to be $\mathcal{K} = 10$. We consider a target (maximum allowed) end-to-end frame error probability of $p_{\text{route}}^{\max} = 10^{-3}$ for both the collector and sensor networks. The frame size is $L = 1000$ bits. The spreading factor is $\kappa = 1.5$, the shipping activity factor is $s = 0.5$ and the wind speed is $w = 0$ m/s. We note that an acoustic signal propagates as a pressure wave whose level is commonly measured in decibel relative to 1 μPa. We adopt that convention; hence, the power levels are expressed in decibel relative to micropascal. We neglect any fixed losses.[‡]

We present an example of a sensor network with 20 000 sensors and 200 collectors deployed uniformly over a circular network of area $\mathcal{A} = 10\,000\ \text{km}^2$. Hence, there are $M_c = 100$ sensors per collector station. Each collector's coverage area is $\mathcal{A}_c \approx 50\ \text{km}^2$. The performance of the collector network is presented in Figure 9. The collector's initial transmit power is $P_c = 118$ dB re μPa, and the bandwidth is $B_c = 4$ kHz. Each collector is equipped with a co-located array with three transmit/receive elements utilising a space–time code that achieves full diversity. The corresponding performance of each collector's cell sensor network is presented in Figure 10. The sensor's initial transmit power is $P_s = 114$ dB re μPa, and the bandwidth is $B_s = 4$ kHz. The sensors are organised into clusters. The cluster size is $N_c = 3$. We assume that $t = 3$ and $r = 1$, that is, the nodes in the transmit cluster collaborate to form a distributed space–time code, but a single node acts as a receiver in the receiving cluster. We also assume that the collector stations and the sensors have the ability to adjust their power levels, so that the sustainable number of hops through the network never exceeds the maximum number of hops given in Equations (7) and (11), respectively. The figures present the sustainable number of hops, operating frequency and transmit power. Clearly, we require the sustainable number of hops to be equal to the maximum number of hops in order to guarantee full connectivity. As we observe from Figures 9 and 10, this is the case for both the collector network and the sensor network. We also observe that the operating frequency for the network of collector stations is different from the operating frequency for the sensor network. For example, the operating frequency for the network of collector stations when the number of collectors is $K = 200$ is about $f_o(d_{\text{col}}) = 14$ kHz. However, the operating frequency for the sensor network when the number of sensors per collector cell is $M_c = 100$ is about $f_o(d_s) = 53$ kHz. Hence, there is a sufficient frequency separation to ensure the operation of the hierarchical sensor network without any cross-interference between the collector network and the sensor network.

4.1. Robustness considerations

Figure 11 presents the sustainable number of sensor cluster-to-cluster hops in a collector cell for different values of the transmit power. The bandwidth is $B_s = 4$ kHz. The end-to-end frame error probability is 10^{-3}. We observe that when the transmit power is $P_s = 114$ dB re μPa, the collector cell is fully connected; hence, data can be gathered from the entire area of the sensor field. However, if the transmit power is reduced to $P_s = 105$ dB re μPa,[§] the network becomes coverage limited when the number of sensors in the collector cell is $M_c \lesssim 37$. In other words, a reduction of the sensors power essentially leads to a reduction in the area of the sensing field of the respective collector cell, at least until the number of sensors in the collector cell is $M_c \lesssim 37$.

The sensitivity of the sustainable number of sensor cluster-to-cluster hops in a collector cell to the carrier frequency is depicted in Figure 12. The transmit power is $P_s = 114$ dB re μPa, and the bandwidth is $B_s = 4$ kHz. The end-to-end frame error probability is 10^{-3}. We observe that when f_o is chosen as the operating frequency, the sensor network provides full connectivity for all values of $M_c < 100$. If the carrier frequency is $f_o \pm 5$ kHz, the sensor network becomes coverage limited when the number of nodes is $M_c \lesssim 10$. Similarly, when the carrier frequency is $f_o \pm 8$ kHz, the sensor network becomes coverage limited when the number of nodes is $M_c \lesssim 35$. This network behaviour is due to the fact that a deviation from the preferred operating frequency f_o causes the SINR to decrease,

[‡]Inclusion of additional frequency-independent losses, and an adjustment of the background noise level to suit a particular environment and provide the necessary SINR margins, will scale the results in absolute value but will not alter the general behaviour.

[§]Recall that the absolute values may scale depending upon the fixed losses and the noise level used for a particular system's link budget.

Trans. Emerging Tel. Tech. (2012) © 2012 John Wiley & Sons, Ltd.
DOI: 10.1002/ett

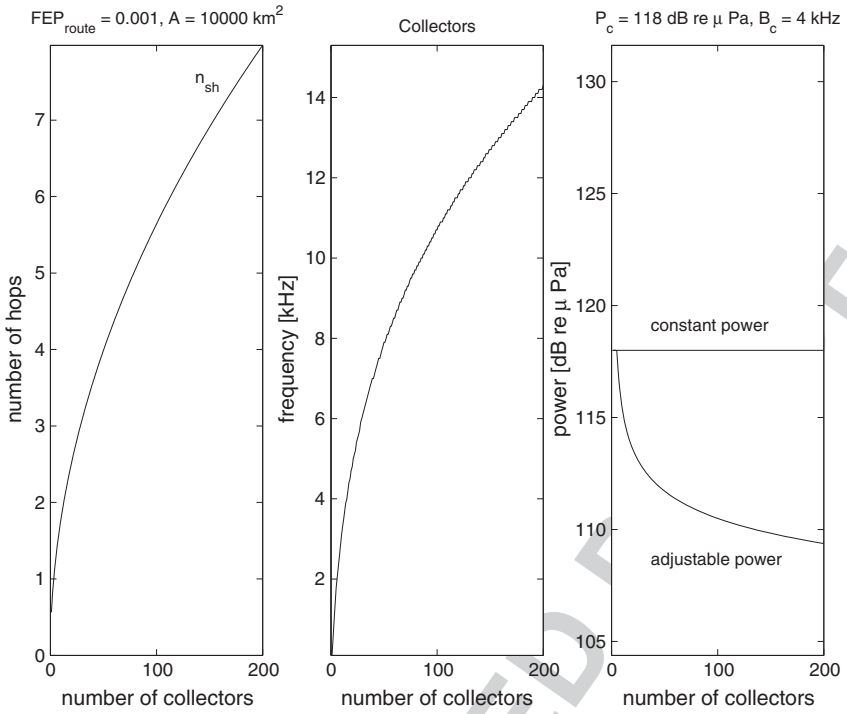

Figure 9. Sustainable number of hops for a uniform network of collector stations with Ricean fading, the operating frequency and the transmit power. The bandwidth is $B_c = 4$ kHz, and the co-located array size is $t = r = 3$.

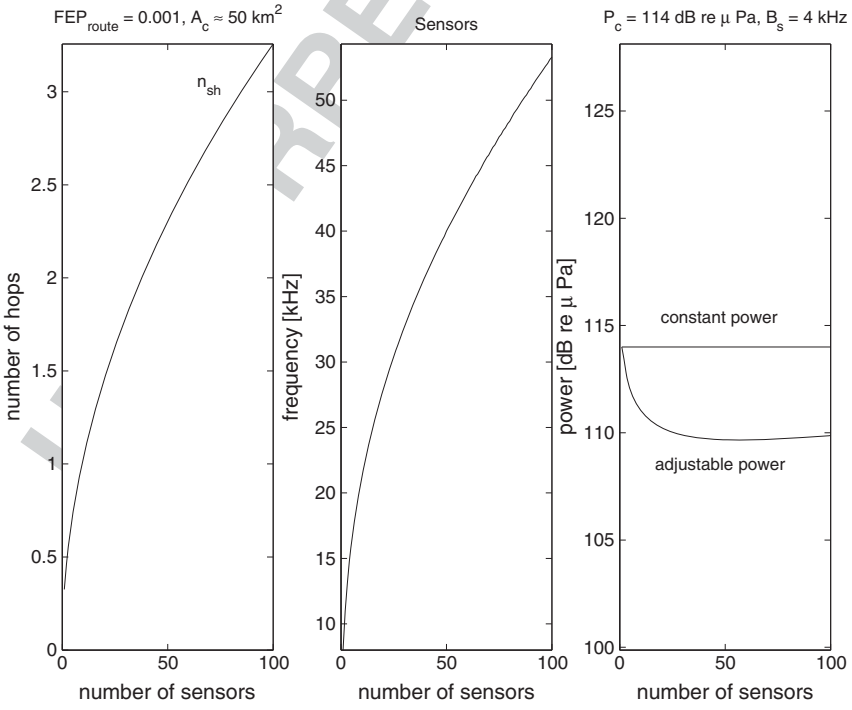

Figure 10. Sustainable number of cluster-to-cluster hops for a uniform distribution of sensors in a collector cell with Ricean fading, the operating frequency and the transmit power. The bandwidth is $B_s = 4$ kHz, the cluster size is $N_c = 3$, $t = 3$ and $r = 1$.

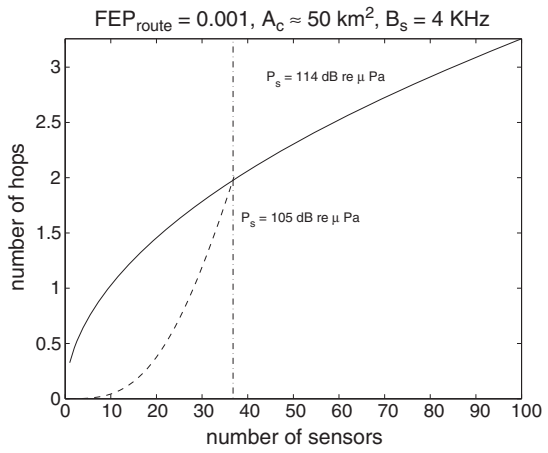

Figure 11. Sustainable number of cluster-to-cluster hops for a uniform distribution of sensors in a collector cell with Ricean fading for various sensors powers. The bandwidth is $B_s = 4$ kHz.

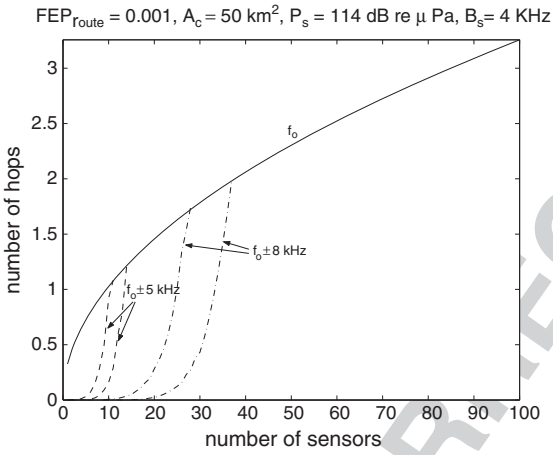

Figure 12. Sustainable number of cluster-to-cluster hops for a uniform distribution of sensors in a collector cell with Ricean fading for various operating frequencies. The power is P_s = 114 dB re μPa, the bandwidth is $B_s = 4$ kHz.

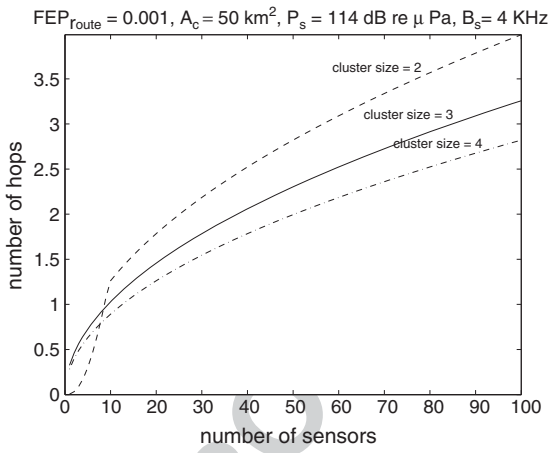

Figure 13. Sustainable number of cluster-to-cluster hops for a uniform distribution of sensors in a collector cell with Ricean fading for various cluster sizes. The power is P_s = 114 dB re μPa, and the bandwidth is $B_s = 4$ kHz.

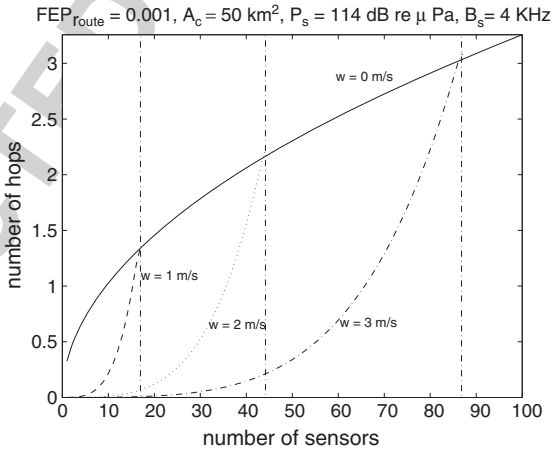

Figure 14. Sustainable number of cluster-to-cluster hops for a uniform distribution of sensors in a collector cell with Ricean fading for various wind speeds. The bandwidth is $B_s = 4$ kHz, and the transmit power is P_s = 114 dB re μPa.

as shown in Figure 6, which results in a decrease in the sustainable number of cluster-to-cluster hops as well.

The impact of the cluster size on the sustainable number of sensor cluster-to-cluster hops in a collector cell is addressed in Figure 13. The transmit power is P_s = 114 dB re μPa, and the bandwidth is $B_s = 4$ kHz. The end-to-end frame error probability is 10^{-3}. We assume that the nodes in the transmit cluster collaborate to form a distributed space–time code, but a single node acts as a receiver in the receiving cluster, that is, $t = N_c$ and $r = 1$. We observe that when the cluster sizes are $N_c = 3$ and $N_c = 4$, the sensor network provides full connectivity for all values of $M_c < 100$. Only when the cluster size is reduced to $N_c = 2$, because of the decreased diversity order, the sensor network becomes coverage limited when the number of nodes is $M_c \lesssim 10$.

Figure 14 illustrates the sustainable number of sensor cluster-to-cluster hops in a collector cell for different wind speeds. The bandwidth is $B_s = 4$ kHz. The end-to-end frame error probability is 10^{-3}. The transmit power is P_s = 114 dB re μPa. We observe that when the wind speed is $w = 0$ m/s, the collector cell is fully connected; hence, data can be gathered from the entire area of the sensor field. However, if the wind speed increases because of an increase in the level of the noise p.s.d., the network becomes coverage limited. As observed in Figure 14, if the wind speed is increased to $w = 1$ m/s, $w = 2$ m/s and $w = 3$ m/s, the network becomes coverage limited when

Trans. Emerging Tel. Tech. (2012) © 2012 John Wiley & Sons, Ltd.
DOI: 10.1002/ett

the numbers of sensors in the collector cell are $M_c \lesssim 17$, $M_c \lesssim 44$ and $M_c \lesssim 87$, respectively. Hence, in a manner analogous to the reduction of the sensors powers, an increase in the wind speed essentially leads to a reduction in the area of the sensing field of the respective collector cell. We note, however, that in practice, the system could operate with a certain margin that would make it possible to raise the sensors powers in order to compensate for the wind-induced increase in the noise p.s.d. level.

5. CONCLUSIONS

We considered a hierarchical sensor network architecture where the sensors and the collector stations operate in distinct layers. The hierarchical architecture was motivated by the property of the acoustic underwater transmission medium that for each transmission distance, there exists an operating frequency for which the narrowband SINR is maximised. The sensors were organised into clusters forming virtual transmit/receive arrays. The collectors were equipped with co-located arrays. A communication-theoretic analysis conducted under the assumption of cluster-to-cluster multihop transmission and Ricean fading, investigated the interdependence of the sustainable number of hops through the network, end-to-end frame error probability, power and bandwidth allocation. Numerical examples showed that there is a sufficient frequency separation to ensure the operation of the hierarchical sensor network without any cross-interference between the collector and sensor networks.

ACKNOWLEDGEMENTS

This work was supported in part by the NSF grant 0831728 and the ONR grant N00014-09-1-0700.

REFERENCES

1. Special issue on underwater wireless communications and networks. *IEEE Journal on Selected Areas in Communications* 2008.
2. *Special Issue on Underwater Networks*, Ad Hoc Networks. Elsevier, 2009.
3. Stojanovic M, Preisig J. Underwater acoustic communication channels: propagation models and statistical characterization. *IEEE Communications Magazine* 2009: 84–89.
4. Stojanovic M. On the relationship between capacity and distance in an underwater acoustic channel. *ACM SIGMOBILE Mobile Computing and Communications Review* 2007; **11**(4): 34–43.
5. Freitag L, *et al.* The WHOI micro-modem: an acoustic communications and navigation system for multiple platforms, In *Proceedings of the IEEE Oceans Conference*, September 2005.
6. Headrick R, Freitag L. Growth of underwater communication technology in the U.S. Navy. *IEEE Communications Magazine* 2009: 80–82.
7. Rice J. SeaWeb acoustic communication and navigation networks, In *Proceedings of the International Conference on Underwater Acoustic Measurements: Technologies and Results*, 2005.
8. Dohler M, Aghvami AH. *Distributed Antennas: the Concept of Virtual Antenna Arrays*, Cooperation in Wireless Networks. Springer, 2006.
9. Dohler M, Gkelias A, Aghvami AH. Capacity of distributed PHY-layer sensor networks. *IEEE Transactions on Vehicular Technology* 2006; **55**: 622–639.
10. Stefanov A, Erkip E. Cooperative space–time coding for wireless networks. *IEEE Transactions on Communications* 2005; **53**(11): 1804–1809.
11. Damen MO, Hammons AR. Delay-tolerant distributed-TAST codes for cooperative diversity. *IEEE Transactions on Information Theory* 2007; **53**: 3755–3773.
12. Tonguz O, Ferrari G. *Ad Hoc Wireless Networks: A Communication-Theoretic Perspective*. Wiley, 2006.
13. Berkhovskikh L, Lysanov Y. *Fundamentals of Ocean Acoustics*. Springer, 1982.
14. Zhang W, Mitra U, Stojanovic M. Analysis of a linear multihop underwater acoustic network. *IEEE Journal of Oceanic Engineering* 2010; **35**: 961–970.
15. Qarabaqi P, Stojanovic M. Statistical modeling of a shallow water acoustic communication channel, In *Proceedings of the Underwater Acoustic Measurements Conference*, Nafplion, Greece, June 2009.
16. Radosevic A, Proakis J, Stojanovic M. Statistical characterization and capacity of shallow water acoustic channels, In *Proceedings of the IEEE Oceans '09 Conference*, Bremen, Germany, May 2009.
17. Benedetto S, Biglieri E. *Principles of Digital Transmission with Wireless Applications*. Kluwer/Plenum, 1999.
18. Hanzo L, Keller T. *OFDM and MC–CDMA: A Primer*. Wiley–IEEE Press, 2006.